International Journal of Biological Macromolecules 87 (2016) 329–340

Contents lists available at ScienceDirect

International Journal of Biological Macromolecules

journal homepage: www.elsevier.com/locate/ijbiomac

Optimizing indomethacin-loaded chitosan nanoparticle size, encapsulation, and release using Box–Behnken experimental design

Mohd Abul Kalam[a], Abdul Arif Khan[a], Shahanavaj Khan[a], Abdulaziz Almalik[b], Aws Alshamsan[a,c,*]

[a] Nanomedicine Research Unit, Department of Pharmaceutics, College of Pharmacy, King Saud University, Riyadh, Saudi Arabia
[b] National Center of Biotechnology, Life Science and Environment Research Institute, King Abdulaziz City of Science and Technology, Riyadh, Saudi Arabia
[c] King Abdullah Institute for Nanotechnology, King Saud University, Riyadh, Saudi Arabia

ARTICLE INFO

Article history:
Received 1 November 2015
Received in revised form 20 January 2016
Accepted 11 February 2016
Available online 15 February 2016

Keywords:
Box–Behnken design
Chitosan
Nanoparticles
Indomethacin

ABSTRACT

Indomethacin chitosan nanoparticles (NPs) were developed by ionotropic gelation and optimized by concentrations of chitosan and tripolyphosphate (TPP) and stirring time by 3-factor 3-level Box–Behnken experimental design. Optimal concentration of chitosan (*A*) and TPP (*B*) were found 0.6 mg/mL and 0.4 mg/mL with 120 min stirring time (*C*), with applied constraints of minimizing particle size (R_1) and maximizing encapsulation efficiency (R_2) and drug release (R_3). Based on obtained 3D response surface plots, factors *A*, *B* and *C* were found to give synergistic effect on R_1, while factor *A* has a negative impact on R_2 and R_3. Interaction of *AB* was negative on R_1 and R_2 but positive on R_3. The factor *AC* was having synergistic effect on R_1 and on R_3, while the same combination had a negative effect on R_2. The interaction *BC* was positive on the all responses. NPs were found in the size range of 321–675 nm with zeta potentials (+25 to +32 mV) after 6 months storage. Encapsulation, drug release, and content were in the range of 56–79%, 48–73% and 98–99%, respectively. *In vitro* drug release data were fitted in different kinetic models and pattern of drug release followed Higuchi-matrix type.

1. Introduction

Chitosan is a cationic hydrophilic linear polysaccharide macromolecule of biological origin. This biocompatible/environment-friendly compound is composed of deacetylated unit (β-(1–4)-linked D-glucosamine) and acetylated unit (*N*-acetyl-D-glucosamine). Chitosan has mucoadhesive and membrane-permeability enhancing properties [1]. It has numerous advantages for mucosal delivery such as biodegradability and low toxicity [2]. It is being used as an excipient in various formulations including micro- and nanoparticles [3]. Multiple methods were reported to prepare chitosan nanoparticles including self-assembly technique through chemical modification, complex coacervation process, emulsion-droplet coalescence, ionotropic gelation and other techniques. Among these techniques, ionotropic gelation [4] is preferred for its relative simplicity, convenience, and the rid of high temperature and organic solvents; hence, sufficient encapsulation of therapeutic agents such as doxorubicin [5], cyclosporine-*A* [6] as well as proteins [7] could be possible.

Phytochemicals like catechins have been fabricated and encapsulated in chitosan-TPP nanoparticles with up to 53% encapsulation efficiency [8]. Chen and Subirade developed chitosan and TPP based nanoparticles to encapsulate a vitamin riboflavin [9]. Also, Desai et al. developed sustained release microspheres of cross linked chitosan loaded with vitamin-C by spray drying [10]. Moreover, the coating of alginate beads with chitosan to encapsulate the living microbial supplements (probiotics) was developed by Le-Tien et al. [11]. During encapsulation of *Lactobacillus acidophilus* and *Lactobacillus casei* in microspheres, chitosan coated alginate beads provided better protection for these two probiotics as compared to poly-L-lysine-coated alginate beads [12]. Similarly, *L. acidophilus*-547 and *L. casei*-01 strains were best protected by chitosan-coated alginate beads [13]. Unsaturated fatty acids functions as neuroprotective, antioxidant, and anti-inflammatory, but they are highly susceptible to oxidative rancidity; therefore, chitosan could be used to stabilized the o/w-emulsions by getting adsorbed on to the oil droplets and form a protective layer by reducing the interfacial tension. Spray dried tuna o/w-emulsion was stabilized by chitosan-lecithin and found oxidative stable as compared to buck oils, hence were found an excellent ω-3 fatty acid compo-

* Corresponding author at: Nanomedicine Research Unit, Department of Pharmaceutics, College of Pharmacy, King Saud University, P.O.Box 2457, Riyadh 11451, Saudi Arabia.
E-mail address: aalshamsan@ksu.edu.sa (A. Alshamsan).

http://dx.doi.org/10.1016/j.ijbiomac.2016.02.033
0141-8130/

nents for the functional foods [14]. Immobilization carriers for enzymes were possible by formulating the chitosan based macro-, micro- and nano-sized particles by precipitation, emulsification, and ionotropic gelation methods, respectively. For example, the highest activity and excellent storage stability of β-galactosidase was found when they were immobilized on chitosan-nanoparticles prepared by ionotropic gelation technique, where sodium sulfate was the gelation agent [15]. Flavors like citral and limonene in emulsion forms were stabilized by sodium dodecyl sulfate-chitosan and were found more effective at hindering the citral oxidation product formation than gum Arabica- stabilized emulsions. Similarly, emulsion of limonene was stabilized by sodium dodecyl sulfate-chitosan, and formation of limonene oxide and carvone were found very low as compared to gum Arabica-stabilized emulsions at pH 3.0. The sodium dodecyl sulfate-chitosan multilayer has ability to form a thick cationic emulsion droplet interface that inhibits the oxidative deterioration of citral and limonene [16].

In this study, we applied ionotropic gelation technique for the preparation of indomethacin-loaded chitosan nanoparticles. Due to the formation of inter- and intramolecular cross-linkages, chitosan gelation occurs when it comes in contact with certain polyanions [5]. In our study, tripolyphosphate was used a cross linker. Although ionotropic gelation of chitosan with tripolyphosphate was firstly reported by Bodmeier et al. [17], our main intention is to apply Box–Behnken design for the optimization of chitosan nanoparticles while assessing the effects of different preparation parameters on their physicochemical characteristics *viz*. particle size, encapsulation and release drug. In this study indomethacin was used as a model drug, however the developed nanoparticles can be used, in principle, to encapsulate hydrophilic or hydrophobic therapeutic agents, bacteria, food, or biochemical ingredients.

2. Materials and methods

2.1. Materials

Indomethacin (Lot No. 134737/42) was purchased from its manufacturer Winlab, UK. High purity, molecular weight 140K-220K, deacetylated chitin (chitosan) and the cross linker tripolyphosphate (TPP) were purchased from Sigma–Aldrich (St. Louis, MO, USA). Acetic acid glacial was purchased from BDH Limited (Poole, England). Dichloromethane and acetonitrile (HiPerSolv CHROMANORM for HPLC grade) were purchased from BDH, PROLABO®, LEUVEN, EC. Purified water was obtained by Milli-Q® water purifier (Millipore, France). All other chemicals used were of analytical grade and the solvents used were of HPLC grade.

2.2. Methods

2.2.1. Experimental design

Response surface methodology was used for optimizing chitosan nanoparticles and investigating the correlation between responses and factors. This study aims to minimizing particle size and maximizing encapsulation and cumulative drug release. Box–Behnken design was employed to evaluate the main effects, interaction effects, and quadratic effects of TPP concentration, chitosan concentration, and stirring time on particle size, encapsulation, and the cumulative drug release. The three-factor three-level design was employed to get the second-order polynomial models using Stat-Ease's Design-Expert-8® (Version 8.0.7.1, Minneapolis, MN, USA). In case of three–four variables Box–Behnken design is chosen, as it needs fewer number of runs than central composite design. A design comprising 17 runs was developed, for which, the nonlinear computer-generated quadratic model can be expresses as:

$$R = b_0 + b_1A + b_2B + b_3C + b_{12}AB + b_{13}AC + b_{23}BC + b_{11}A^2 + b_{22}B^2 + b_{33}C^2$$

where R is response, b_0 is intercept, b_1–b_{33} are regression coefficients computed from the observed values of R from experiments, and A, B and C are independent variables. The terms (AB, AC *and* BC) and (A^2, B^2 *and* C^2) represent the interaction and quadratic terms, respectively [18,19]. TPP concentration (A), chitosan concentration (B) and stirring time (C) are the independent variables. Their concentration ranges, presented in Table 1 with low, medium and high levels, were selected on the basis of preliminary experiments in developing the nanoparticles. Average particle size (R_1), encapsulation efficiency (R_2), and cumulative drug release were the dependent variables. The amount of TPP (A), chitosan (B) and stirring duration (C) were used for 17 experimental formulations and their observations on the dependent variables are presented in Table 2.

2.2.2. Optimization, data analysis, and validation of the applied model

ANOVA was used for the statistical validation of the polynomial equations created by Design-Expert®. All the responses were fitted to linear, second order, and quadratic models then evaluated in terms of statistical significance of coefficients and R^2 squared values. Different possibilities were tried to find out the constituents for the optimized nanoparticles. The software obtained three-dimensional response surface plots. A total 5 checkpoint formulations were selected for the validation of the chosen experiment and equations. The checkpoint (optimized) formulations were formulated and characterized for the selected responses. The observed response values were compared with the predicted values and prediction errors (%) were calculated. The linear correlation and residual plots between observed and predicted responses were obtained.

2.2.3. Formulation of indomethacin chitosan nanoparticles

Chitosan nanoparticles were prepared by ionic gelation method. Briefly, by the addition of TPP aqueous solution to the diluted acetic acid–chitosan solution according to the method reported by Calvo et al. [4]. Chitosan was dissolved in acetic acid aqueous solution to reach the concentrations 0.2, 0.35, 0.6 and 1.2 mg/mL. Indomethacin was dissolved in 0.25 mL of dichloromethane and mixed with the chitosan solution. Thereafter, 5 mL TPP of different concentrations (0.2, 0.4, 0.5, 0.8, and 1.0 mg/mL) were added to 10 mL chitosan solution at the addition rate of 1.5 mL/min, under magnetic stirring at 500 rpm for 60, 90, 120 and 180 min at room temperature. The levels of three factors in Table 1, the low, medium and high level of variables were chosen and given to the Design Expert software, the software resulted different runs those are in Table 2, All the runs with different ratios of excipients in Table 2 were formulated and evaluated for the selected three physicochemical responses, out of these only 5 formulations were chosen and the amount of their ingredients were slightly modified to check any adverse effects on the responses, these 5 formulations were found stable in terms of physicochemical characteristics so were selected as optimized formulations.

2.2.4. Particle size analysis and zeta-potential measurements

Photon correlation spectroscopy was employed to determine particle size using Zetasizer Nano-Series (Nano-ZS, Malvern Instruments Limited, Worcestershire, UK). Samples were appropriately

Table 1
Variables in Box–Behnken design for indomethacin chitosan nanoparticles.

Factor	Actual and coded levels used for the nanoparticles		
	Low (−1)	Medium (0)	High (+1)
A = tripolyphosphate concentration (mg/mL)	0.20	0.60	1.00
B = chitosan concentration (mg/mL)	0.10	0.65	1.20
C = stirring time (min)	60	120	180

Dependent variables	Constrains
R_1 = particle size (nm)	Minimize
R_2 = encapsulation efficiency (%)	Maximize
R_3 = cumulative drug release (%)	Maximize (for sustained release)

Table 2
Observed responses in Box–Behnken design for indomethacin chitosan nanoparticles.

Batch	Indomethacin chitosan nanoparticles					
	Independent variables			Dependent variables (responses)		
	A (mg/mL)	*B* (mg/mL)	*C* (min)	R_1 (nm) (mean ± SD)	R_2 (%) (mean ± SD)	R_3 (%) (mean ± SD)
1	1.00	1.20	120.00	425.55 ± 11.94	65.54 ± 6.28	54.25 ± 6.57
2	1.00	0.65	180.00	455.64 ± 12.08	49.62 ± 4.78	48.45 ± 6.25
3*	0.60	0.65	120.00	401.27 ± 10.26	82.25 ± 6.25	73.49 ± 7.35
4	0.60	1.20	60.00	354.62 ± 12.38	68.35 ± 4.35	52.09 ± 4.56
5	0.60	1.20	180.00	528.85 ± 13.19	65.62 ± 6.45	57.92 ± 5.12
6*	0.60	0.65	120.00	435.37 ± 11.58	80.35 ± 9.24	70.68 ± 7.16
7	0.20	0.65	60.00	504.29 ± 14.57	60.48 ± 4.24	62.35 ± 6.24
8	0.60	0.10	60.00	602.78 ± 19.56	61.65 ± 5.25	64.55 ± 6.25
9	0.20	0.65	180.00	398.29 ± 13.34	64.63 ± 5.28	51.65 ± 5.45
10	0.20	0.10	120.00	511.45 ± 13.47	53.34 ± 3.95	57.85 ± 4.95
11*	0.60	0.65	120.00	425.85 ± 15.25	75.15 ± 8.52	69.28 ± 7.24
12	1.00	0.10	120.00	701.51 ± 17.54	61.38 ± 5.69	46.95 ± 4.52
13*	0.60	0.65	120.00	405.19 ± 16.28	79.29 ± 10.25	65.75 ± 8.72
14	0.60	0.10	180.00	585.53 ± 15.78	56.35 ± 7.24	45.34 ± 5.69
15	0.20	1.20	120.00	415.25 ± 13.50	72.08 ± 6.18	51.34 ± 6.23
16*	0.60	0.65	120.00	400.55 ± 13.45	75.85 ± 9.28	59.97 ± 5.49
17	1.00	0.65	60.00	452.95 ± 14.52	48.23 ± 4.52	52.85 ± 6.25

* Indicates the center point of the design.

diluted with Milli-Q® water (Millipore, France) before measurement. Zeta-potentials of the formulated nanoparticles were also determined using the same instrument. Samples were diluted with Milli-Q® water and by keeping the dispersant dielectric constant 78.5 for water, the electrophoretic mobility was determined at 25 °C. Zeta potential was calculated using the software DTS Version 4.1 (Malvern, Worcestershire, UK). Each experiment was performed in triplicate.

2.2.5. Morphology of nanoparticles by transmission electron microscopy (TEM)

The surface morphology and structure of optimized chitosan based nanoparticles of indomethacin (F3) was evaluated using JEOL TEM (JEM-2100F). TEM analysis was carried out under light microscopy operating at 100 KV capable of point-to-point resolution. Combination of bright field imaging at increasing magnification and of diffraction modes was used to reveal the structure and size of the nanoparticles [20]. To perform TEM analysis, the suspension of nanoparticles was diluted further with purified water. Afterwards, copper grid coated with carbon film was placed over the drop, stained with 2% solution of phosphotungstic acid, and observed after drying at room temperature [18].

2.2.6. Encapsulation efficiency and drug loading

The encapsulation efficiency (EE) was determined by measuring the concentration of free drug in the dispersion medium. A known dilution of the indomethacin nanoparticles dispersion was prepared with double distilled water and was centrifuged at 13,500 rpm by cooling centrifuge (PRISM-R, Labnet International Inc. Edison, NJ, USA) for 30 min at 10 °C. The amount of encapsulated drug into the nanoparticles was the difference between the total amount used to prepare the nanoparticles and the amount that was found in the supernatant [21].

For drug loading (DL) the supernatant in case of encapsulation determination was removed and the nanoparticles sediment (precipitant) was washed by distilled water and dispersed in 5 mL mixture of chloroform and dichloromethane at 1:1 ratio in a 10 mL volumetric flask. To ensure complete drug extraction, the mixture was sonicated by ultrasonicator (Model-3510, Branson Ultrasonic Corporation) for 30 min and the volume was made up to 10 mL with chloroform. The resulting solution was centrifuged at 13,500 rpm at 10 °C for 30 min. Drug concentration in the supernatant was analyzed by HPLC [22]. Both the experiments were performed in triplicate and calculation was done [23] using the straight line equation, $y = 150696x - 18053$; $R^2 = 0.9959$, according to Eq. . and Eq. (2).

$$\text{Encapsulation efficiency}\,(\%) = \left(\frac{W_1 - W_2}{W_1}\right) \times 100 \quad (1)$$

$$\text{DL}\,(\%) = \left(\frac{\text{Amount of drug in NPs sediment (mg)}}{\text{Amount of drug added}\,(mg) + \text{Total amount of excipients (mg)}}\right) \times 100 \quad (2)$$

where "W_1" is the weight of total actual amount of drug used in the formulation and the "W_2" is the amount of free drug analyzed in the supernatant.

2.2.7. Swelling behavior study

Swelling behavior was conducted as a function of time the [24,25], where a dry weight of chitosan nanoparticles sample (M_1)

was immersed in phosphate buffer saline (pH 7.4) at room temperature for different time intervals up to 24 h. At each time point, chitosan nanoparticles were collected and mounted on filter paper to soak the excess buffer then weighed (M_2) and the degree of swelling was calculated according to Eq. (3):

$$\text{Degree of swelling}\,(\%) = \left(\frac{M_2 - M_1}{M_1}\right) \times 100 \quad (3)$$

The swelling behavior of chitosan nanoparticles was also conducted in external environment as a function of pH. The nanoparticles were first immersed in purified water at room temperature to the equilibrium state and weighed (W_{Eq}). Then, immersed in PBS at various pH values (1.5, 3.5, 7.2, 8.5 and 9.5) for 24 h. At each pH, the sample was taken and soaked on filter paper to remove extra buffer then weighed (W_{pH}) and the degree of swelling was calculated according to Eq. (4).

$$\text{Degree of swelling}\,(\%)\,\text{at pH} = \left(\frac{W_{pH}}{W_{Eq}}\right) \times 100 \quad (4)$$

2.2.8. In vitro *drug release studies*

In vitro release of indomethacin from chitosan nanoparticles was performed in PBS (pH 7.4). The indomethacin-loaded nanoparticles were diluted in PBS reaching final indomethacin concentration of 100 μg/mL in each tubes. Each sample was put in Eppendorf tubes of 2.0 mL capacity, which were placed on floating slab and kept in shaking water bath at 37 ± 0.5 °C and were allowed to be shaken at a rate of 100 rpm. At predetermined time points (1, 2, 3, 4, 5, 6, 7, 8, 9, 10, 11 and 12 h) after starting incubation, a set of three Eppendorf tubes were taken out from the water bath and centrifuged at 13,500 rpm for 30 min; thereafter, supernatants were collected and concentrations of released indomethacin were analyzed by HPLC at 241 nm detection wavelength as described in Ref. [22]. Cumulative drug release data were analyzed by using different kinetic model equations, where M_0 is the initial amount of drug (*i.e.*, 100%), M_t the amount of drug remaining at a particular time '*t*', *k* is the rate constant, and *n* is diffusion exponent that indicates the release mechanism. From the slope and intercept of the plot of obtained through different kinetic models, kinetic parameters *n* and *k* were calculated [24,26].

2.2.9. Stability studies

The five optimized chitosan nanoparticles were stored away from direct sunlight for 6 months in glass vials at 25 °C. The changes in the particles size, zeta potential, encapsulation efficiency, and drug content of the stored nanoparticles were investigated after 3 and 6 months.

3. Results and discussions

In the present study we have chosen a lipophilic drug, indomethacin, to encapsulate into chitosan-TPP nanoparticles as a model drug, and evaluated the morphology of the produced nanoparticles by transmission electron microscopy (TEM), particle size, polydispersity, zeta potential, encapsulation efficiency, drug loading, swelling behavior of chitosan nanoparticles in water, and *in-vitro* drug release. Our results have given indications that the developed nanoparticles by ionic gelation method using Box–Behnken Design® software for optimization would be fruitful for successful encapsulation of many therapeutic agent for several drug delivery systems including oral, transdermal, and ocular.

3.1. Fitting of data in to the selected model

A direct correlation was observed between chitosan concentration and particle size. An increase in particle size (301–650 nm, depending on the TPP concentration, 0.2–1.0 mg/mL) was observed with increasing chitosan concentration. At 1.2 mg/mL chitosan concentration, particle size ranged from 354 nm to 528.85 nm depending upon the TPP concentration (0.2–1.0 mg/mL) and the stirring duration (60–180 min). At the same concentration of chitosan, the variation in encapsulation efficiency and drug release were found in the range of 65.54–72.08% and 51.34–65.75%, respectively, depending upon the TPP concentration and stirring time (Table 2). On fitting the observed response variables in different models, the quadratic model was found to be the best-fitted model for all the three responses (Table 3). The coefficient values for TPP, chitosan, and stirring time duration transmit the comparative and significant effects of these factors on particle size, encapsulation efficiency, and release of indomethacin from the developed chitosan nanoparticles (Table 4a), where the values of standard error for different coefficients suggested the non-linear nature of these links (quadratic) in all the cases of response variables. In the regression equations for responses, a positive value specifies a synergistic effect on the optimization, while a negative value directs an antagonistic effect between the factors and the responses [27]. It can be seen in Table 4a that the independent variables *A*, *B* and *C* have synergistic effects on the response R_1 (particle size), while TPP (*A*) is having antagonistic effects on the responses R_2 (encapsulation efficiency) and R_3 (drug release).

3.1.1. Interaction effects of factors on the responses

In regression equations, coefficients with more than one factor and with higher order terms indicate the interaction terms and the quadratic relationships, respectively, as well as suggesting the non-linear relationship between the factors and responses [28]. These interaction effects of the two factors (TPP and chitosan concentrations) by keeping stirring time as constant can be observed in Fig. 1. The interaction effect of *A*, *B* and *C* were found to have a synergistic on responses R_1 (particle size, Eq. (5) in Table 3). While factor *A* (TPP) has a negative impact on the responses R_2 (encapsulation, Eq. (6) in Table 3) and R_3 (drug release, Eq. (7) in Table 3). The interaction of *AB* was found to have an inverse relationship with the responses R_1 and R_2 but a positive effect on the drug release (R_3) with a high magnitude on particle size (R_1). The effect of *AC* was synergistic on particle size (R_1) and on drug release (R_3), while the same combination was showing a negative impact of encapsulation (R_2). The interaction effect of *BC* was found positive on the all the three dependent variables (R_1, R_2 and R_3). For the response R_1 (particle size), the quadratic effects of *A*, *B* and *C* were positive (with highest magnitude) at any instance, whereas the quadratic effects of *A*, *B* and *C* were found to have a negative impact on encapsulation (R_2) as well as on drug release (R_3) from chitosan nanoparticles.

Moreover, the closeness between the adjusted and predicted R-squared values for all the responses for the regression equations shows the statistical significance and validity of these equations for the optimization of chitosan nanoparticles. It was found from the regression equations (Table 4a) that the particle sizes are principally affected by the TPP as well chitosan concentration, while the encapsulation efficiency and drug release were mainly affected by the chitosan concentration and stirring time duration.

For responses R_1 (particle size), R_2 (encapsulation efficiency) and R_3 (cumulative drug release) the model *F*-values of 6.16, 7.43 and 7.50 respectively, implies that the model was significant for all the three chosen responses (Table 4b). For responses R_1, R_2 and R_3, there were only a 1.28%, 0.75% and 0.73% chances respectively, that the "model *F*-values" this large could occur due to noises. The values of "Probability > *F*" and less than 0.0500 indicate the model terms were significant, therefore, in case of R_1, the terms *B* and B^2, in case of R_2, the terms *B*, A^2 and C^2 and in case of R_3 the terms *C*, *BC*, A^2, B^2 and C^2 were found significant model terms. The values greater than 0.1000 indicate the model terms were not significant. The "lack of

Table 3
Regression analysis results and ANOVA for the response surface quadratic model of responses R_1, R_2 and R_3.

Models	Indomethacin chitosan nanoparticles (CS-NP-IND)						Remarks
	R squared	Adjusted *R* squared	Predicted *R* squared	SD	%CV	Adequate precision for ANOVA	
Response R_1 (Particle size)							
Linear model	0.8612	0.8379	0.8246	7.68	7.45	3.973	–
Second order	0.8793	0.8494	0.8398	6.96	8.78	4.565	–
Quadratic model	0.9178	0.8974	0.8856	5.93	9.77	8.235	Suggested
Response R_2 (Encapsulation efficiency)							
Linear model	0.8659	0.8457	0.8244	6.83	5.69	3.548	–
Second order	0.8811	0.8789	0.8547	7.58	4.97	4.267	–
Quadratic model	0.9285	0.8908	0.8752	4.84	7.39	7.359	Suggested
Response R_3 (cumulative drug release)							
Linear model	0.8643	0.8306	0.8193	8.88	5.86	5.245	–
Second order	0.8997	0.8725	0.8558	9.05	6.58	4.354	–
Quadratic model	0.9873	0.9676	0.9479	4.15	7.24	7.093	Suggested

Regression eaquations in terms of coded factors for indomethacin loaded chitosan nanoparticles:

$R_1 = 413.0 + 25.63A + 84.62B + 6.75C - 45.0AB + 27.25AC + 47.75BC + 17.4A^2 + 82.4B^2 + 21.65C^2$ . . . . . Eq. (5)

$R_2 = 78.20 - 3.25A + 4.88B - 0.37C - 3.75AB - 0.75AC + 0.5BC - 11.35A^2 - 4.18B^2 - 11.6C^2$ . . . . . Eq. (6)

$R_3 = 67.20 - 2.63A + 0.25B - 3.63C + 3.5AB + 1.75AC + 6.0BC - 8.22A^2 - 6.97B^2 - 5.73C^2$ . . . . . Eq. (7)

Table 4a
Quadratic model and the coefficients for the drug release from formulation, encapsulation efficiency and particle size for indomethacin chitosan nanoparticles.

Terms	Particle size (nm)			Encapsulation efficiency (%)			Cumulative drug release (%)		
	Coefficient	SE	Range[a]	Coefficient	SE	Range[a]	Coefficient	SE	Range[a]
Constants	413.0	20.54	(364.63) to (461.77)	78.20	2.16	(73.08) to (83.32)	67.20	1.86	(62.81) to (71.59)
Tripolyphosphate (A)	25.63	16.24	(−12.78) to (64.03)	−3.25	1.71	(−7.30) to (0.80)	−2.63	1.47	(−6.09) to (0.84)
Chitosan (B)	84.62	16.24	(−123.03) to (−46.22)	4.88	1.71	(0.83) to (8.92)	0.25	1.47	(−3.22) to (3.72)
Stirring time (C)	6.75	16.24	(−31.65) to (45.15)	−0.37	1.71	(−4.42) to (3.67)	−3.63	1.47	(−7.09) to (−0.16)
Tripolyphosphate × Chitosan ($A \times B$)	−45.00	22.97	(−99.31) to (9.31)	−3.75	2.42	(−9.47) to (1.97)	3.50	2.07	(−1.41) to (8.41)
Tripolyphosphate × Stirring time ($A \times C$)	27.25	22.97	(−27.06) to (81.56)	−0.75	2.42	(−6.47) to (4.97)	1.75	2.07	(−3.16) to (6.66)
Chitosan × Stirring time ($B \times C$)	47.75	22.97	(−6.56) to (102.06)	0.50	2.42	(−5.22) to (6.22)	6.00	2.07	(1.09) to (10.91)
Tripolyphosphate × Tripolyphosphate (A^2)	17.40	22.39	(−35.53) to (70.33)	−11.35	2.36	(−16.93) to (−5.77)	−8.22	2.02	(−13.01) to (−3.44)
Chitosan × Chitosan (B^2)	82.40	22.39	(29.47) to (135.33)	−4.10	2.36	(−9.68) to (1.48)	−6.97	2.02	(−11.76) to (−2.19)
Stirring time × Stirring time (C^2)	21.65	22.39	(−31.28) to (74.58)	−11.60	2.36	(−17.18) to (−6.08)	−5.73	2.02	(−10.51) to (−0.94)

[a] The range indicates the lower and upper value of coefficients at 95% confidence interval.

Table 4b
Analysis of variance for response surface quadratic model.

Terms	Particle size (R_1)			Encapsulation efficiency (R_2)			Cumulative drug release (R_3)		
	F-values	*p*-values	Remarks	*F*-values	*p*-values	Remarks	*F*-values	*p*-values	Remarks
Quadratic model	6.16	0.0128	Significant	7.43	0.0075	Significant	7.50	0.0073	Significant
Tripolyphosphate (A)	2.52	0.1563		3.44	0.1060		3.36	0.1096	
Chitosan (B)	27.15	0.0012		7.83	0.0266		6.49	0.9380	
Stirring time (C)	0.17	0.6913		0.032	0.8628		6.36	0.0397	
$A \times B$	3.83	0.0913		2.20	0.1812		2.99	0.1273	
$A \times C$	1.40	0.2754		0.079	0.7868		0.62	0.4560	
$B \times C$	4.34	0.0756		0.069	0.8011		9.84	0.0165	
A^2	0.60	0.4645		22.59	0.0021		17.73	0.0040	
B^2	13.57	0.0078		2.97	0.1287		13.11	0.0085	
C^2	0.95	0.3621		22.96	0.0020		8.94	0.0202	
Lack of fit	18.04	0.0087	Significant	4.86	0.0804	Not significant	0.039	0.9881	Not significant

fit *F*-values" 18.04 for R_1 and 4.86 for R_2 implies the lack of fit was significant and there were only 0.87% and 8.04% chances for R_1 and R_2 respectively, that a "lack of fit *F*-values" this large might occured due to noises. Similarly, for R_3 the "lack of fit *F*-value" 0.04 implies the lack of fit was not significant relative to the pure error. There was around 98.81% chance that a "lack of fit *F*-value" this large could occur due to noise and the non-significant lack of fit was good.

3.1.2. Validation of the applied model

For the graphical optimization of IND-chitosan-NPs, a three dimensional (3D) response surface plots were obtained by the used software, which was fruitful to determine the interaction effects of independent variables on dependent variables. The 3D plots display the influences of two factors on a particular response, and the third factor remained constant. Influence of TPP and chitosan concentrations and stirring duration on particle size, encapsulation and drug release of IND-chitosan-NPs are represented graphically in Fig. 1. The optimized chitosan-nanoparticles were chosen on the basis of minimizing the particle size, maximizing encapsulation and drug release by using the limitations and constraints. Upon through understanding and evaluation of responses, five chitosan-nanoparticles were found to have the criteria of optimized formulations. For all five checkpoint formulations, the evaluated values of particle size, encapsulations and drug release were found satisfactorily good (Table 5). Prediction errors (%) assured the validity of the obtained regression equations. Linear correlation plots of observed versus predicted responses (Fig. 2) indicated that the

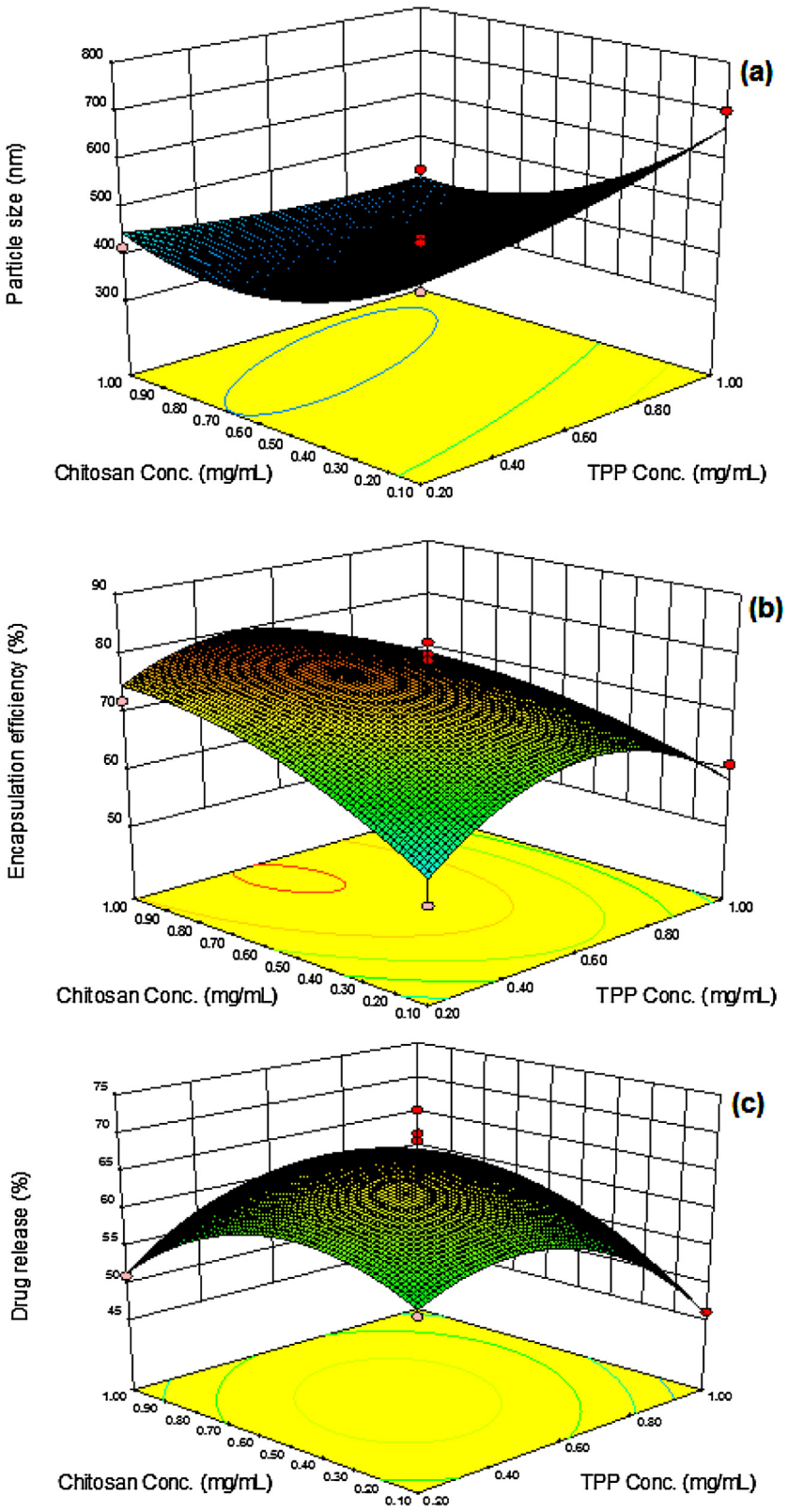

Fig. 1. Three-dimensional response surface plots for the graphical optimization of chitosan-NPs showing interaction effect of cross-linker, TPP (A) and polymer, chitosan (B) on particle size (a), encapsulation efficiency (b) and on drug release (c) for chitosan-TPP based nanoparticles.

scatter of the residuals *versus* actual values signified the spread of dependent variables under this experimental situations.

The RSM model summary statistics focusses on the model maximizing the "adjusted *R*-squared" and the "predicted *R*-squared" values. The model *F*-values 6.15, 7.72 and 6.87 for R_1, R_2 and R_2 respectively, implies that the model is significant. There are only 1.28%, 0.67% and 0.94% chances for R_1, R_2 and R_2 respectively, that a model *F*-values, these large could occur due to noise. The values

Table 5
Composition of checkpoint formulations of indomethacin chitosan nanoparticles, the predicted and experimental values of responses and percentage prediction error.

Optimized formulation composition and stirring time (*A*: *B*: *C*)	Response variables	Experimental value	Predicted value	Percentage prediction error
0.20: 0.35: 180 (F1)	R_1 (particle size, nm)	451.21	432.35	+4.179
	R_2 (encapsulation, %)	62.65	59.75	+4.628
	R_3 (cumulative drug release, %)	51.25	48.65	+5.073
0.50: 0.20: 60 (F2)	R_1 (particle size, nm)	301.25	315.65	−2.396
	R_2 (encapsulation, %)	59.35	61.58	−3.757
	R_3 (cumulative drug release, %)	62.28	60.15	+3.421
0.40: 0.60: 120 (F3)	R_1 (particle size, nm)	401.54	398.85	+0.669
	R_2 (encapsulation, %)	81.25	82.56	−1.612
	R_3 (Cumulative drug release, %)	75.75	72.54	+4.238
0.80: 1.2: 90 (F4)	R_1 (particle size, nm)	650.55	654.75	−0.646
	R_2 (encapsulation, %)	63.47	65.45	−3.169
	R_3 (cumulative drug release, %)	53.56	55.15	−2.968
1.0: 0.35: 120 (F5)	R_1 (particle size, nm)	425.75	415.52	+2.403
	R_2 (encapsulation, %)	68.25	66.25	+2.556
	R_3 (cumulative drug release, %)	62.15	58.25	+6.275

of "probability > *F*" less than 0.050 indicated that model terms are significant and values greater than 0.100 indicated that the model terms are not significant. In case of R_1, the independent variables *B*, B^2 are significant model terms, in case of R_2, variables *B*, A^2, C^2 are significant model terms while in case of R_3 variables *C*, *BC*, A^2, B^2, C^2 are significant model terms. The lack of fit *F*-values 0.18, 0.43 and 0.04 for R_1, R_2 and R_3, respectively, implies that the lack of fit is non-significant relative to the pure error. The chances in the lack of fit *F*-values for R_1, R_2 and R_3 were found to be 85.25%, 96.2% and 98.62%, respectively (quadratic models), these large might occured due to noise. Non-significant lack of fit is good, so the model used was found to be fit. The regression analysis results and ANOVA for the response surface of models for responses R_1, R_2 and R_3 are presented Table 3. In all cases the "predicted *R*-squared" was found in the reasonable agreement with the "adjusted *R*-quared". Moreover, the adequate precision measures the signal to noise ratio, and a ratio greater than 4 is desirable. Here the ratio of 8.235 (for R_1), 7.359 (for R_2) and 7.093 (for R_3) indicates an adequate signal, hence this model could be used to navigate the response surface design space.

3.2. Formulation of chitosan nanoparticles

The chitosan-nanoparticles were prepared by ionic gelation technique where the drop by drop addition of TPP aqueous solution to chitosan solution resulted in the formation of chitosan-NPs. Primary trials were done for the selection of the optimum ratios of TPP and chitosan for the formulation of chitosan-NPs. Three kinds of phenomena were observed during addition of TPP in to chitosan: solution, aggregates and opalescent suspension. The appearance of opalescence was further investigated for the formation of nanoparticles. The formation of particles was thought to be the result of the interaction between the negatively charged groups of the TPP and the positively charged amino groups of chitosan.

The characterization results suggested that the particle size were increasing with increasing chitosan concentration. The fact that the generation chitosan-TPP nanoparticles was only feasible at specified concentrations of chitosan and TPP [4] was clear in this experiment that to circumvent the development of any microparticles, the TPP and chitosan concentration were kept not more than 1.0 mg/mL and 1.2 mg/mL, respectively. In acidic conditions, there is an ectrostatic repulsion between chitosan molecules because of the presence of protonated amino groups of chitosan, and an inter chain hydrogen bonding interactions between chitosan molecules are also existing. Under a specific concentration of chitosan this inter chain hydrogen bonding attraction and intermolecular electrostatic repulsion are in equilibrium [29]. Hence, in the concentration range (Table 5), as the chitosan concentration increases, chitosan molecules approach each other, resulting in a partial escalation in intermolecular cross-linking, so a little larger nanoparticles were obtained (Table 5). It was found that chitosan at 0.4 mg/mL concentration formed stable nanoparticles at small mass ratio of TPP: chitosan (0.2:0.3) at an optimum stirring time of 120 min (Table 5), which might be due to the fact that at the decreased chitosan concentration, the intermolecular distance increases, causing a reduced intermolecular cross-linking between chitosan molecules and at the same time enhancement in cross-linking density between chitosan molecules, in other words an increase in the molar ratio of TPP and chitosan repeating units [30,31]. An acceptable average particle size range (301–650 nm), encapsulation efficiency (59–78%) and drug release (51–75%) in response to changes in magnetic stirring time. The optimum average particle size, 401 nm with highest encapsulation efficiency (81.25%) and highest drug release (75.75%) was found (F3) at 0.2 mg/mL cross-linker (TPP) and 0.6 mg/mL polymer (chitosan) concentrations and 120 min of stirring duration (Table 5). Moreover, the optimized formulations were selected based on the criteria of attaining the maximum value of encapsulation and cumulative drug release as well as minimizing the particle size by applying numerical point prediction optimization method of the Box–Behnken Design Expert software®. The formulation composition with TPP, chitosan and stirring time (Section 2.2.3) were found to fulfill requisites of an optimized chitosan nanoparticles as F1–F5. The experimental observed values of particle size, encapsulation and cumulative drug released presented by F1–F5 found in agreement with the predicted values of the three responses generated by the software, suggesting that the optimized formulation was trustworthy and rational.

3.3. Morphological characterization of chitosan-nanoparticles (TEM)

Transmission electron microscopy (TEM) observation has shown that the nanoparticles were discrete and isolated in their distribution and having spherical morphology with solid dense structure (Fig. 3). The size of nanoparticles (F3) seemed to be smaller significantly when assessed with TEM (350–450 nm) comparatively when analyzed by the photon correlation spectroscopy (PCS), Malvern Zetasizer Instrument (301–675 nm). This obvious variance in the sizes of nanoparticles might be due to dehydration of the chitosan nanoparticles during their drying on copper grid for the imaging by TEM. Moreover, PCS measures the hydrodynamic diameter of particles or any solid or hollow spherical structures, including hydrodynamic layers that may develop around the surfaces of hydrophilic nanoparticles as they are composed of chitosan and tri-polyphosphates (both are hydrophilic in nature), which in

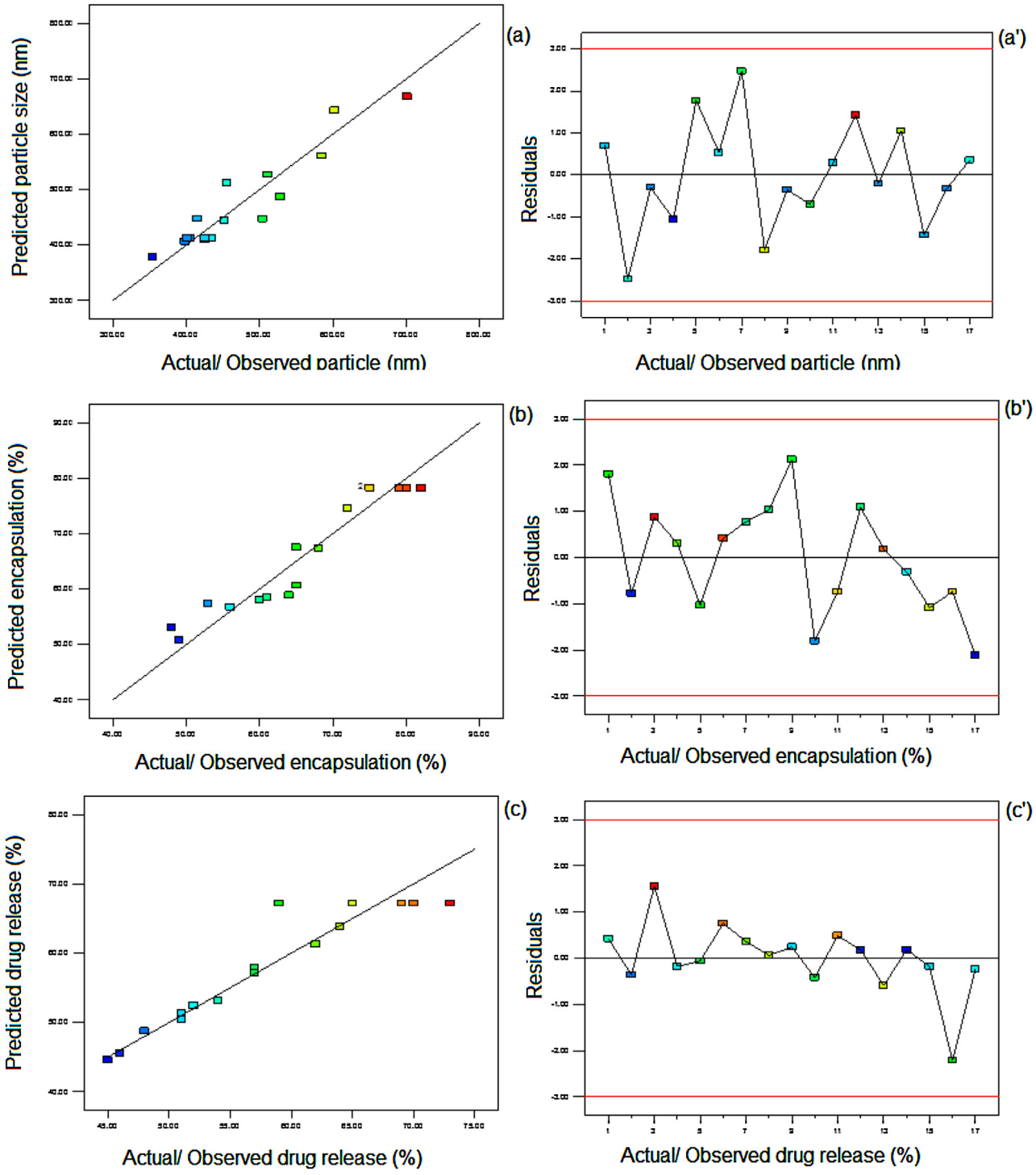

Fig. 2. Linear correlation plots (a–c) between observed/actual and predicted values and corresponding residual plots (a'–c') for the three responses *i.e.*, particle size (nm), encapsulation (%) and drug release (%) for chitosan-TPP based nanoparticles. Scattered of the residuals *versus* actual values represent the spread of the dependent variables under the experimental conditions.

turn causing an over approximation of the sizes of nanoparticles [18,32].

3.4. Particle size analysis, polydispersity and zeta-potentials

The results of formulations and characterizations indicate that NPs prepared with TPP-chitosan in ratio 0.2:0.3 (F3) was found the best formulations among the five optimized formulations (F1–F5) with an average particle size of 401 nm. All the optimized formulations has shown monomodal size distribution. With increasing chitosan concentration an increase in the average particle size were found in the range of 301–650 nm. The polydispersity index (PDI) of the all the formulations (F1–F5) was found low, indicating that the developed chitosan-nanoparticles are homogeneously dispersed in the dispersion medium. An increase in the values (0.115–0.215) of PDI was observed with increasing concentration of chitosan in the five optimized formulations (Table 6). It is remarkable that the PCS by Malvern Zetasizer Instrument measures the hydrody-

Table 6
Particle size, polydispersity, zeta potential, drug encapsulation and loading efficiencies of chitosan nanoparticles of varying weight ratios of CS and TPP (mean ± SD, $n = 3$).

Formulations (TPP: CS)	Z-average (nm)	PDI	Zeta-potential (mV)	Encapsulation (%EE)	Drug Loading (%DL)	Swelling diffusion kinetics at pH 7.4	
						n-values	*K*-values
F1 (0.20: 0.35)	449.52 ± 15.75	0.145 ± 0.075	+36.05 ± 2.18	62.65 ± 3.74	12.85 ± 1.78	0.0874	0.4636
F2 (0.50: 0.20)	301.85 ± 18.45	0.115 ± 0.029	+28.14 ± 3.23	59.35 ± 2.64	10.23 ± 1.26	0.0989	0.5245
F3 (0.40: 0.60)	401.54 ± 14.25	0.198 ± 0.054	+31.25 ± 3.45	81.25 ± 4.75	21.51 ± 1.46	0.0759	0.4025
F4 (0.80: 1.20)	658.25 ± 12.65	0.215 ± 0.036	+27.14 ± 4.26	62.47 ± 3.12	14.25 ± 1.08	0.0575	0.3049
F5 (1.00: 0.35)	430.95 ± 10.56	0.146 ± 0.018	+26.19 ± 2.48	68.25 ± 4.43	16.72 ± 1.35	0.0857	0.4543

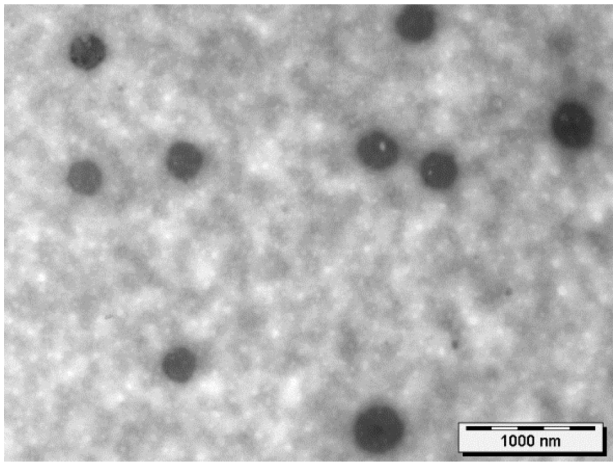

Fig. 3. Transmission electron microphotographs of chitosan-NP-INDO (F3) presenting solid dense spherical structure in the nano-range.

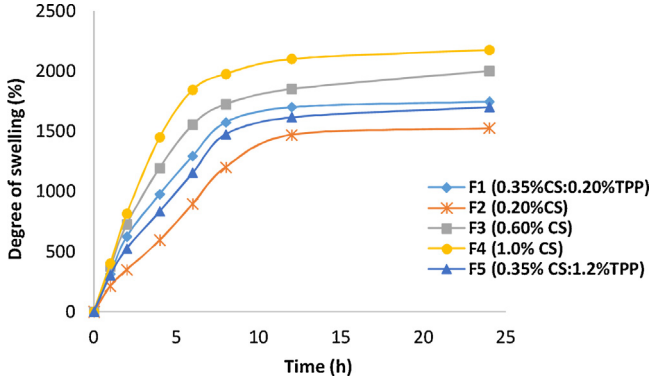

Fig. 4. Swelling behavior of chitosan nanoparticles with time in water at room temperature.

namic diameter of nanoparticles (F3, 400–445 nm) which is higher than their size assessed with TEM (F3, 300–350 nm) particularly because of high swelling capacity of chitosan-nanoparticles due its highly hydrophilic nature. Therefore, actual average sizes of the developed chitosan-nanoparticles could considered to be significantly smaller than they appeared in PCS measurement [18]. All the chitosan nanoparticles were found to have positive zeta potential values (Table 6). The positive values of zeta potential are due to the presence of cationic chitosan on the surface of nanoparticles. It was found that the absolute zeta potential values decreased with increasing the TPP concentration which is an agreement with the previously results of Fan et al. [30]. A high magnitude of absolute zeta potentials are indicative that the developed chitosan-nanoparticles are having good dispersion stability.

3.5. Encapsulation and drug loading efficiencies

The mean encapsulation efficiencies (%EE) and the mean drug loading capacities (%DL) of the optimized (F1–F5) formulations are presented in Table 6. Lower value of %EE and %DL in case of F2 might be due to the lower concentration of chitosan and minimum stirring time duration. There are differences in the formulations F1 and F5, while both are having same amount of chitosan, but the stirring time period was high in case of F5, prolonged stirring might be the reason for the leaching of the encapsulated drug. F3 is having good %EE and %DL capacity as formulated with optimum concentration of chitosan and TPP with 120 min of stirring duration, having satisfactory drug release in the 12 h *in vitro* release study, so it was considered as the best formulation amongst the five optimized chitosan-nanoparticles. F4 is also having good encapsulation and drug loading, but here the particle sizes are very high as compared to F3 even at short duration of stirring.

3.6. Swelling behavior and swelling kinetics

The degree of swelling of all the chitosan nanoparticles increases sharply up to 6 h incubation, while it increases slowly with less extent up to 24 h incubation. Fig. 4, represents the swelling kinetics of chitosan nanoparticles in water at room temperature and at 7.4 pH. They reach the equilibrium state after 6 h and up to 24 h. The nanoparticles with higher concentration of chitosan polymer exhibited higher degree of swelling (F3 and F4) as compared to those with lower concentration (F1, F2 and F5) of the same polymer, that means the degree of swelling exhibited a systematic trend in according to the composition, *i.e.*, the degree of swelling is directly proportional to the concentration of chitosan and the higher degrees of swelling of chitosan based nanoparticles might be due to the hydrophilic nature of the polymer matrix. The nature of water distribution into the chitosan nanoparticles was determined by using Fick's law of diffusion [33]:

$$\ln F = \ln K + n \ln t \quad (8)$$

where W_t and W_e are the quantity of water absorbed by the chitosan nanoparticles at time '*t*' and at equilibrium, *K* is a constant characteristic of the matrix networks and '*n*' is an exponent that estimates water diffusion mode, *F* is the fraction of drug release. The plot between ln *F* versus ln *t* gives a straight line, where the intercept gives the value of constant *K* and from the slope of straight line values of '*n*' was calculated. When the value of $n = 0.5$, it indicates a Fickian diffusion mechanism where sorption is the diffusion controlled, when it (*n*) is $0.5 < n < 1$, it is an anomalous non-Fickian diffusion and attributes to the process of water-sorption. Fig. 5, represents the application of Fick's law of diffusion in terms of the equations (Eq. (8)) for chitosan-nanoparticles and diffusion parameters are presented in Table 7. The values of '*n*' indicated that all the chitosan nanoparticles exhibit a non-Fickian diffusion. Hence, it could be assumed that the diffusion of water into the nanoparticles matrix is not controlled, however it rely on the process of water sorption, which in turn depends on the structure of the matrix network and pathways of water sorption. Moreover, lowest values

Table 7
Drug release model study by fitting *in vitro* release study.[a]

Release models	Equations	Formulation F1		Formulation F2		Formulation F3		Formulation F4		Formulation F5	
		R^2 value	*n*-value	R^2 value	*n*-value	R^2 value	*n*-value	R^2 value	*n*-value	R^2 value	*n*-value
Zero order	$M_0 - M_t = kt$	0.9366	–	0.9183	–	0.9472	–	0.9728	–	0.9625	–
First order	$\ln M_t = \ln M_0 + kt$	0.9577	–	0.9432	–	0.9757	–	0.9821	–	0.9834	–
Higuchi's matrix	M_0-$M_t = kt^{1/2}$	0.9912	0.0823	0.9858	0.0396	0.9853	0.0553	0.9930	0.0259	0.9970	0.0387
Korsmeyer–Peppas	$\log (M_0 - M_t) = \log k + n \log t$	0.9909	–	0.9845	–	0.9847	–	0.9722	–	0.9917	–
Hixson–Crowell	$M_0^{1/3} - M_t^{1/3} = k_s t$	0.9512	–	0.9358	–	0.9660	–	0.9793	–	0.9774	–

[a] M_0 is the initial drug amount (100%, when represented as percentage); M_t the amount of drug remaining at a particular time; k the rate constant; t is the time and n is diffusion exponent.

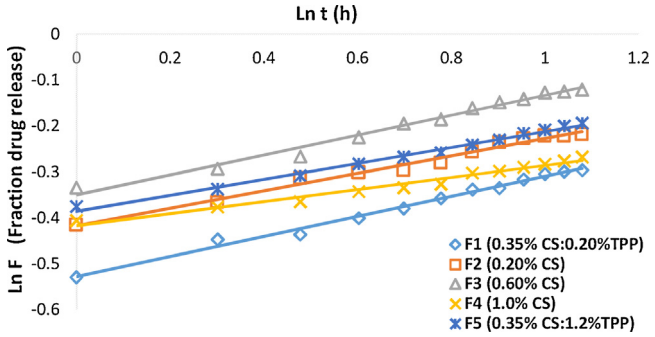

Fig. 5. The plots between Ln *F* and Ln *t* for the chitosan and tripolyphosphate (TPP) based nanoparticles of indomethacin.

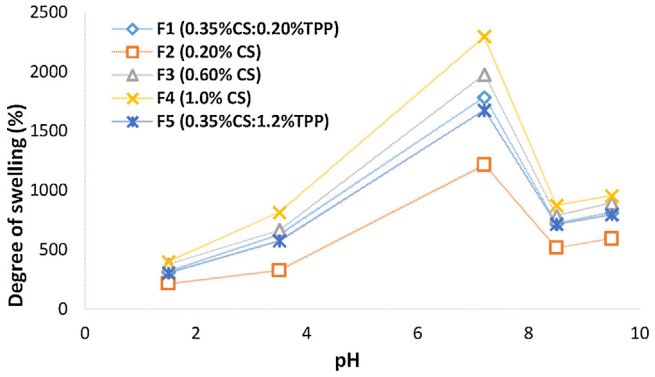

Fig. 6. Effect on the degree of swelling at different pH values in water at room temperature for the chitosan and tripolyphosphate (TPP) based nanoparticles of indomethacin.

of '*n*' and '*K*' were found in case of F4 (higher concentration chitosan) and the significant differences in swelling diffusion kinetics parameters were found for other formulations (F1, F2, F3 and F5) as compared to F4 (Table 7). These outcomes specify the contribution of higher concentration of chitosan in F4 during the sorption process which generated an extra water pathways in the matrix network.

Fig. 6, represents the effect of pH on degree of swelling for nanoparticles based on different ratios of chitosan and TPP. It was found that there was no substantial change in degree of swelling in the pH range of 1.5–3.5. Conversely, a very clear effect of pH was found in the pH range of 3.5–8.5, where the degree of swelling increased abruptly at pH 7.2 and decreased suddenly at pH range 8.5–9.5, which might be associated with the sensitivity of chitosan in the presence of salts in the PBS solutions. The addition of salt modifies the ionic distribution inside the matrix of chitosan nanoparticles, causing an alteration in the number of dissociated groups in the network matrix, hence changes the absolute electrical charges on the surface. Thus modification in the network electrical state was assumed to be the basic reason for swelling

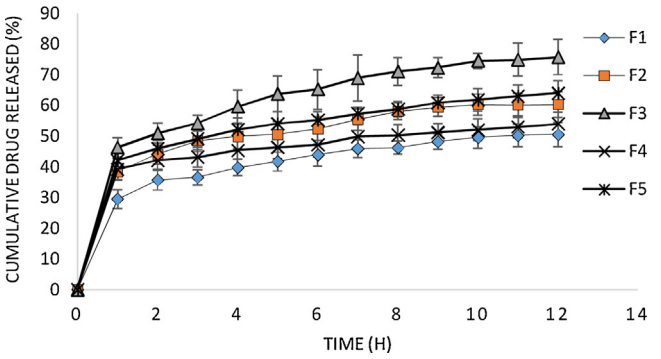

Fig. 7. Indomethacin release from chitosan-nanoparticles in phosphate buffer saline at pH 7.4.

and deswelling of nanoparticles, depending up on whether there is an increase or decrease in the electrical repulsions [34]. So, this deswelling behavior at higher pH was governed by the intramolecular electrostatic contributions [35,36]. It can be seen from the plot that pH sensitivity of chitosan-TPP nanoparticles is directly proportional to the chitosan concentration. The network matrix of chitosan contains many pH-ionizable groups, therefore a variation in pH definitely modify the network electrical state, resulting electrostatic repulsion in the network which in turn affect the swelling behavior of chitosan-NPs. In other words this pH-dependent behavior can be attributed to the protonation of the amino groups ($-NH_2$) on the chitosan network, causing the increased electric density and repulsion forces between cross-linked chitosan networks.

3.7. In vitro *drug release study*

In vitro release profile of indomethacin from chitosan-nanoparticles in PBS (pH 7.4) are presented in Fig. 7. The release of drug from chitosan-nanoparticles should be sustained and it is important, as it would allow for a prolonged retention of the drug at the target surface, would increase drug bioavailability and prolong therapeutic effect. The release of indomethacin from the chitosan-nanoparticles follow a biphasic pattern with an initial burst and rapid release followed by a slower release period. Up to 60 min the rapid release phase was lasted in all the five optimized formulations and in this duration about 30–50% of the indomethacin was found to be released from the chitosan-nanoparticles, which is an agreement with the study of drug-loaded chitosan nanoparticles [37]. The initial fast release of indomethacin from chitosan-NP at pH 7.4 (simulated intestinal fluid) was thought due to the fast dissolution of the drug molecules adsorbed on the surface of nanoparticles which diffuse out easily in the initial phase of incubation, moreover large specific surface area of nanoparticles could adsorb the drug, hence initial burst release was assumed due the desorption of indomethacin from the surface of chitosan-nanoparticles [38]. After the initial burst release, the release rate slow down that might be due to the changed mechanism of drug *i.e.*, diffusion of

Table 8
Evaluation of particle size, zeta potential, drug encapsulation, drug content remained and drug release of CS-nanoparticles of indomethacin during storage for 6 months at 25 °C (Mean ± SD, $n = 3$).

Formulations	Z-Average (nm)	Zeta-potential (mV)	Encapsulation (%EE) ± SD	Drug content (%) ± SD	Cumulative drug release (%) ± SD
At initial time					
F1	449.52 ± 15.75	+36.05 ± 2.18	62.65 ± 3.74	100.00	51.25 ± 1.78
F2	301.85 ± 18.45	+28.14 ± 3.23	59.35 ± 2.64	100.00	62.28 ± 1.26
F3	401.54 ± 14.25	+31.25 ± 3.45	81.25 ± 4.75	100.00	75.75 ± 1.46
F4	658.25 ± 12.65	+27.14 ± 4.26	62.47 ± 3.12	100.00	53.56 ± 1.08
F5	430.95 ± 10.56	+26.19 ± 2.48	68.25 ± 4.43	100.00	62.15 ± 1.35
At 3rd month					
F1	459.25 ± 14.15	+33.26 ± 2.13	60.52 ± 2.43	99.15 ± 0.56	50.01 ± 1.08
F2	315.25 ± 15.78	+27.15 ± 3.12	57.24 ± 3.17	98.97 ± 1.87	60.12 ± 2.01
F3	408.85 ± 15.45	+30.15 ± 2.35	80.44 ± 4.75	99.65 ± 1.01	74.72 ± 1.25
F4	670.62 ± 18.57	+26.35 ± 2.56	61.15 ± 3.54	99.31 ± 1.05	51.28 ± 1.07
F5	440.59 ± 16.25	+25.65 ± 3.08	66.12 ± 3.28	99.12 ± 1.02	60.23 ± 1.23
At 6th month					
F1	464.23 ± 16.24	+32.15 ± 2.16	58.26 ± 2.45	98.34 ± 0.51	48.27 ± 1.05
F2	321.26 ± 15.42	+26.56 ± 3.08	56.21 ± 1.97	98.01 ± 1.25	58.54 ± 1.42
F3	414.15 ± 17.25	+29.59 ± 2.05	79.23 ± 2.75	99.14 ± 1.51	73.39 ± 1.26
F4	675.56 ± 18.29	+26.05 ± 2.65	59.55 ± 2.35	98.99 ± 1.23	50.15 ± 1.35
F5	445.25 ± 14.68	+25.01 ± 2.73	62.58 ± 3.12	98.89 ± 1.58	59.54 ± 2.15

indomethacin through the matrix of chitosan. The overall "rate" of drug release (*i.e.*, fraction of drug content of the nanoparticles released at a particular time point) increased as the drug encapsulation in the nanoparticles increased (81.25% encapsulation in F3, shown highest drug release, 51% even at 1st hour of study). It may be assumed that the differences in the release of indomethacin among the chitosan-nanoparticles at pH 7.4 (SIF) was because of the differences in encapsulation of drug in chitosan-nanoparticles (F1-F5). So, encapsulation of drug efficiently control the rate of drug release. From the *in vitro* results it can be assumed that the chitosan nanoparticles would reveal a similar sustained release *in vivo*, which is an indication that that chitosan-nanoparticles could be considered as a controlled drug delivery system for indomethacin.

3.7.1. Mechanisms of drug release and data analysis

When the indomethacin loaded chitosan nanoparticles exposed with the release medium, the aqueous phase imbibes into the nanoparticles, causes the hydrolytic degradation of the chitosan molecules and thus release of drug occurs. Various mathematical models have been reported to quantify the drug release from different delivery carriers where the drug is homogeneously distributed throughout the carrier system with an initial drug concentration higher than their solubility in the carrier material *i.e.*, monolithic dispersions [39]. The most important and suitable theory of such kind of release mechanism was developed by Higuchi [40], and the principle of his approach was based on a pseudo steady-state assumption for the simplicity reasons. Under the particular condition when the concentration gradient is almost constant, provided the initial drug concentration within the system is much higher than the solubility of the drug, Higuchi derived another very simple relationship between the release rate of the drug and the square root of time in the case of planar devices and in later stage of his research, he extrapolated his theory to spherical geometry and derived an implicit mathematical model equation for the quantitative determination of the released drug [41].

The drug release behavior from all the five optimized indomethacin loaded chitosan nanoparticles were subjected to fit in to various drug release kinetic models and it was found that overall curve fitting (Table 7**)** represented the drug release from chitosan-nanoparticles followed Highuchi-matrix kind of release mechanism as evidenced by their higher values of coefficients of determination (R^2) of the straight line equations (Table 7). The fitting in to kinetic models was based on minimizing the differences between practical and theoretical values. From the slopes of straight lines of the fitting equations, the '*n*-values' were calculated that were found in the range of 0.0259–0.0823, which suggested a Fickian diffusion release mechanism, that described the sustained release of Indomethacin from the chitosan-NPs up to 12 h, which was being supported by Mullers' theory "in the drug-enriched core model, the drug release is membrane-controlled and governed by the Fick's law of diffusion" as the chitosan make a surrounding layer around the drug molecules and behave like a membrane. The initial burst release was found predominantly whereas a slow, sustained and constant phase of drug release were found, which may indicated a probable clarification for the burst effect [42]. Since, normally the diffusion-controlled release of drug illustrates a significantly higher release rate initially which is might be due to the small diffusion pathways at the starting time-points [43]. Therefore, the bursting phenomenon may be attributed to a normal diffusion-controlled drug release.

3.8. Stability study results

The physicochemical stability studies for a period of 6 months on the optimized chitosan-nanoparticles were performed. After 3 and 6 months of storage at 25 °C, an increase in the particle sizes ranged 8.73–14.71 nm (F1), 13.40–19.41 nm (F2), 7.31–12.61 nm (F3), 12.37–17.31 nm (F4), 9.64–14.30 nm (F5) and decrease in the zeta-potentials ranged 2.79–3.90 (F1), 0.99–1.58 (F2), 1.10–1.66 (F3), 0.79–1.09 (F4), 0.54–1.18 (F5) were observed. The percent encapsulation of indomethacin was lowered by 2.13–4.39 (F1), 2.11–3.14 (F2), 0.81–2.02 (F3), 1.32–2.92 (F4), 2.13–5.67 (F5), reduction in the percent drug contents were found in the range of 0.85–1.66 (F1), 1.03–1.99 (F2), 0.35–0.86 (F3), 0.69–1.01 (F4), 0.88–1.11 (F5) and decrease in percent drug released was found in the range of 1.24–2.98 (F1), 2.16–3.74 (F2), 1.03–2.36 (F3), 2.28–3.44 (F4), 1.92–2.61 (F5) (Table 8). The particle size analysis carried out on the storage formulations after 3 and 6 months, a small increase in the diameter were found, which might be due to swelling and water adsorption behavior of chitosan-NPs. This swelling nature and degradation of chitosan in the aqueous phase might be the reason for drug expulsion from NPs and hence there were decreased encapsulation efficiency and drug release from chitosan-nanoparticles after long term storage [44].

4. Conclusions

Using ionotropic gelation method, good average sized positively charged chitosan-nanoparticles with high encapsulation efficiency; satisfactory drug release and good storage stabil-

ity properties could be produced and optimized by using a three-factor, three-level Box–Behnken design. High magnitudes of zeta-potential of the NPs indicated a stable dispersive nature of the developed chitosan-NPs.The quantitative effect of the chosen independent factors at different levels to achieve minimum particles size, and maximum encapsulation of drug and its release would be predicted using polynomial equations. The observed linearity between actual and predicted values of the responses suggested the predictive ability of the response surface methodology (RSM). Hence, a high degree of prediction achieved by RSM is relatively efficient in optimizing the chitosan-NPs as controlled and sustained drug-delivery systems that exhibit nonlinearity in the responses. The chitosan-NPs based controlled delivery system developed in this study would have potential applications and could serve as an optimal model to encapsulate any hydrophilic or hydrophobic therapeutic agent, vitamins, probiotics, enzeymes, flavors, fatty acids, antimicrobial agents and peptides etc.

Conflict of interest

The authors declare no competing financial interest.

Acknowledgment

This project was funded by the Research Groups Program (Research Group number RG-1436-027), Deanship of Scientific Research, King Saud University, Riyadh, Saudi Arabia.

References

[1] S. Papadimitriou, D. Bikiaris, K. Avgoustakis, E. Karavas, M. Georgarakis, Chitosan nanoparticles loaded with dorzolamide and pramipexole, Carbohydr. Polym. 73 (2008) 44–54.
[2] A. Rampino, M. Borgogna, P. Blasi, B. Bellich, A. Cesaro, Chitosan nanoparticles: preparation, size evolution and stability, Int. J. Pharm. 455 (2013) 219–228.
[3] M. Dash, F. Chiellinia, R.M. Ottenbriteb, E. Chiellini, Chitosan—a versatile semi-synthetic polymer in biomedical applications, Prog. Polym. Sci. 36 (2011) 981–1014.
[4] P. Calvo, C. Remunan-Lopez, J.L. Vila-Jato, M.J. Alonso, Chitosan and chitosan/ethylene oxide-propylene oxide block copolymer nanoparticles as novel carriers for proteins and vaccines, Pharm. Res. 14 (1997) 1431–1436.
[5] K.A. Janes, M.P. Fresneau, A. Marazuela, A. Fabra, M.J. Alonso, Chitosan nanoparticles as delivery systems for doxorubicin, J. Control Release 73 (2001) 255–267.
[6] A.M. De Campos, A. Sanchez, M.J. Alonso, Chitosan nanoparticles: a new vehicle for the improvement of the delivery of drugs to the ocular surface. Application to cyclosporin A, Int. J. Pharm. 224 (2001) 159–168.
[7] S. Al-Qadi, A. Grenha, D. Carrion-Recio, B. Seijo, C. Remunan-Lopez, Microencapsulated chitosan nanoparticles for pulmonary protein delivery: in vivo evaluation of insulin-loaded formulations, J. Control Release 157 (2012) 383–390.
[8] B. Hu, C. Pan, Y. Sun, Z. Hou, H. Ye, X. Zeng, Optimization of fabrication parameters to produce chitosan-tripolyphosphate nanoparticles for delivery of tea catechins, J. Agric. Food Chem. 56 (2008) 7451–7458.
[9] L. Chen, M. Subirade, Chitosan/beta-lactoglobulin core-shell nanoparticles as nutraceutical carriers, Biomaterials 26 (2005) 6041–6053.
[10] K.G. Desai, C. Liu, H.J. Park, Characteristics of vitamin C encapsulated tripolyphosphate-chitosan microspheres as affected by chitosan molecular weight, J. Microencapsul. 23 (2006) 79–90.
[11] C. Le-Tien, M. Millette, M.A. Mateescu, M. Lacroix, Modified alginate and chitosan for lactic acid bacteria immobilization, Biotechnol. Appl. Biochem. 39 (2004) 347–354.
[12] W. Krasaekoopt, B. Bhandari, H. Deeth, The influence of coating materials on some properties of alginate beads and survivability of microencapsulated probiotic bacteria, Int. Dairy J. 14 (2004) 737–743.
[13] W. Krasaekoopt, B. Bhandari, H.C. Deeth, Survival of probiotics encapsulated in chitosan-coated alginate beads in yoghurt from UHT- and conventionally treated milk during storage, LWT-Food Sci. Technol. 39 (2006) 177–183.
[14] U. Klinkesorn, P. Sophanodora, P. Chinachoti, D.J. McClements, E.A. Decker, Stability of spray-dried tuna oil emulsions encapsulated with two-layered interfacial membranes, J. Agric. Food Chem. 53 (2005) 8365–8371.
[15] E. Biro, A.S. Nemeth, C. Sisak, T. Feczko, J. Gyenis, Preparation of chitosan particles suitable for enzyme immobilization, J. Biochem. Biophys. Methods 70 (2008) 1240–1246.
[16] D. Djordjevic, L. Cercaci, J. Alamed, D.J. McClements, E.A. Decker, Chemical and physical stability of citral and limonene in sodium dodecyl sulfate-chitosan and gum arabic-stabilized oil-in-water emulsions, J. Agric. Food Chem. 55 (2007) 3585–3591.
[17] R. Bodmeier, H.G. Chen, O. Paeratakul, A novel approach to the oral delivery of micro- or nanoparticles, Pharm. Res. 6 (1989) 413–417.
[18] M. Abul Kalam, Y. Sultana, A. Ali, M. Aqil, A.K. Mishra, I.A. Aljuffali, A. Alshamsan, Part I: development and optimization of solid-lipid nanoparticles using Box–Behnken statistical design for ocular delivery of gatifloxacin, J. Biomed. Mater. Res. A 101 (2013) 1813–1827.
[19] S.K. Motwani, S. Chopra, S. Talegaonkar, K. Kohli, F.J. Ahmad, R.K. Khar, Chitosan-sodium alginate nanoparticles as submicroscopic reservoirs for ocular delivery: formulation, optimisation and in vitro characterisation, Eur. J. Pharm. Biopharm. 68 (2008) 513–525.
[20] S. Shafiq, F. Shakeel, S. Talegaonkar, F.J. Ahmad, R.K. Khar, M. Ali, Development and bioavailability assessment of ramipril nanoemulsion formulation, Eur. J. Pharm. Biopharm. 66 (2007) 227–243.
[21] A. Debrassi, C. Burger, C.A. Rodrigues, N. Nedelko, A. Slawska-Waniewska, P. Dluzewski, K. Sobczak, J.M. Greneche, Synthesis, characterization and in vitro drug release of magnetic *N*-benzyl-*O*-carboxymethylchitosan nanoparticles loaded with indomethacin, Acta Biomater. 7 (2011) 3078–3085.
[22] L. Novakova, L. Matysova, L. Havlikova, P. Solich, Development and validation of HPLC method for determination of indomethacin and its two degradation products in topical gel, J. Pharm. Biomed. Anal. 37 (2005) 899–905.
[23] J. Liu, T. Gong, C. Wang, Z. Zhong, Z. Zhang, Solid lipid nanoparticles loaded with insulin by sodium cholate-phosphatidylcholine-based mixed micelles: preparation and characterization, Int. J. Pharm. 340 (2007) 153–162.
[24] T.S. Anirudhan, D. Dilu, S. Sandeep, Synthesis and characterisation of chitosan crosslinked-β-cyclodextrin grafted silylated magnetic nanoparticles for controlled release of Indomethacin, J. Magn. Magn. Mater. 343 (2013) 149–156.
[25] H.M. Nizam El-Din, S.G. Abd Alla, A.W.M. El-Naggar, Swelling and drug release properties of acrylamide/carboxymethyl cellulose networks formed by gamma irradiation, Radiat. Phys. Chem. 79 (2010) 725–730.
[26] X. Wei, N. Sun, B. Wu, C. Yin, W. Wu, Sigmoidal release of indomethacin from pectin matrix tablets: effect of in situ crosslinking by calcium cations, Int. J. Pharm. 318 (2006) 132–138.
[27] J. Hao, X. Fang, Y. Zhou, J. Wang, F. Guo, F. Li, X. Peng, Development and optimization of solid lipid nanoparticle formulation for ophthalmic delivery of chloramphenicol using a Box-Behnken design, Int. J. Nanomed. 6 (2011) 683–692.
[28] Z. Rahman, A.S. Zidan, M.J. Habib, M.A. Khan, Understanding the quality of protein loaded PLGA nanoparticles variability by Plackett–Burman design, Int. J. Pharm. 389 (2010) 186–194.
[29] G. Qun, W. Ajun, Effects of molecular weight, degree of acetylation and ionic strength on surface tension of chitosan in dilute solution, Carbohydr. Polym. 64 (2006) 29–36.
[30] W. Fan, W. Yan, Z. Xu, H. Ni, Formation mechanism of monodisperse, low molecular weight chitosan nanoparticles by ionic gelation technique, Colloids Surf. B Biointerfaces 90 (2012) 21–27.
[31] J. Berger, M. Reist, J.M. Mayer, O. Felt, N.A. Peppas, R. Gurny, Structure and interactions in covalently and ionically crosslinked chitosan hydrogels for biomedical applications, Eur. J. Pharm. Biopharm. 57 (2004) 19–34.
[32] S. Prabha, W.Z. Zhou, J. Panyam, V. Labhasetwar, Size-dependency of nanoparticle-mediated gene transfection: studies with fractionated nanoparticles, Int. J. Pharm. 244 (2002) 105–115.
[33] A. Roy, J. Bajpai, A.K. Bajpai, Dynamics of controlled release of chlorpyrifos from swelling and eroding biopolymeric microspheres of calcium alginate and starch, Carbohydr. Polym. 76 (2009) 222–231.
[34] A. Fernandez-Nieves, A. Fernandez-Barbero, F.J. de las Nieves, B. Vincent, Motion of microgel particles under an external electric field, J. Phys.: Condensed Matter 12 (2000) 3605–3614.
[35] T. Lopez-Leon, E.L. Carvalho, B. Seijo, J.L. Ortega-Vinuesa, D. Bastos-Gonzalez, Physicochemical characterization of chitosan nanoparticles: electrokinetic and stability behavior, J. Colloid Interface Sci. 283 (2005) 344–351.
[36] C. Xiao, H. Li, Y. Gao, Preparation of fast pH-responsive ferric carboxymethylcellulose/poly(vinyl alcohol) double-network microparticles, Polym. Int. 58 (2009) 112–115.
[37] Y. Boonsongrit, A. Mitrevej, B.W. Mueller, Chitosan drug binding by ionic interaction, Eur. J. Pharm. Biopharm. 62 (2006) 267–274.
[38] S.A. Agnihotri, N.N. Mallikarjuna, T.M. Aminabhavi, Recent advances on chitosan-based micro- and nanoparticles in drug delivery, J. Control Release 100 (2004) 5–28.
[39] N. Faisant, J. Siepmann, J.P. Benoit, PLGA-based microparticles: elucidation of mechanisms and a new simple mathematical model quantifying drug release, Eur. J. Pharm. Sci. 15 (2002) 355–366.
[40] T. Higuchi, Rate of release of medicaments from ointment bases containing drugs in suspension, J. Pharm. Sci. 50 (1961) 874–875.
[41] T. Higuchi, Mechanism of sustained-action medication. theoretical analysis of rate of release of solid drugs dispersed in solid matrices, J. Pharm. Sci. 52 (1963) 1145–1149.
[42] J. Siepmann, A. Gopferich, Mathematical modeling of bioerodible, polymeric drug delivery systems, Adv. Drug Deliv. Rev. 48 (2001) 229–247.
[43] J. Siepmann, F. Lecomte, R. Bodmeier, Diffusion-controlled drug delivery systems: calculation of the required composition to achieve desired release profiles, J. Control Release 60 (1999) 379–389.
[44] A.A. Badawi, H.M. El-Laithy, R.K. El Qidra, H. El Mofty, M. El dally, Chitosan based nanocarriers for indomethacin ocular delivery, Arch. Pharm. Res. 31 (2008) 1040–1049.